IEEE Access
Multidisciplinary | Rapid Review | Open Access Journal

Received June 9, 2021, accepted June 27, 2021, date of publication July 12, 2021, date of current version August 3, 2021.

Digital Object Identifier 10.1109/ACCESS.2021.3096331

Analysis and Mitigation of the Communication Delay Impacts on Wind Farm Central SSI Damping Controller

MOHSEN GHAFOURI[1], (Member, IEEE), ULAS KARAAGAC[2], (Member, IEEE), ILHAN KOCAR[3], (Senior Member, IEEE), ZHAO XU[2], (Senior Member, IEEE), AND EVANGELOS FARANTATOS[4], (Senior Member, IEEE)

[1]Security Research Center, Concordia Institute for Information Systems Engineering (CIISE), Concordia University, Montreal, QC H3G 1M8, Canada
[2]Department of Electrical Engineering, The Hong Kong Polytechnic University, Hong Kong
[3]Department of Electrical Engineering, Polytechnique Montréal, Montreal, QC H3T 1J4, Canada
[4]Electric Power Research Institute (EPRI), Palo Alto, CA 94304, USA

Corresponding author: Ulas Karaagac (ulas.karaagac@polyu.edu.hk)

This work was supported in part by the Le Fonds de recherche du Québec–Nature et technologies (FRQNT) under Grant 2022-NC-300985, and in part by the Hong Kong Research Grant Council for the Research Project under Grant 25223118.

ABSTRACT The use of supplementary controllers for mitigating subsynchronous interaction (SSI) in series compensated DFIG-based wind farms is quite promising due to high effectiveness and low cost. Implementation of such a controller requires effective communications between individual turbines and the wind farm controller, where the control performance is very much affected by the communication delays involved. This paper delivers the first detailed analysis on the impact of communication delays on SSI damping controller performance. A novel algorithm is proposed to calculate the stability delay margin (SDM) of the closed-loop system based on Rekasius Substitution and Guardian Map Theorem with the advantage of reduced computational burden particularly for high-order systems. Based on the proposed algorithm, the impacts of wind farm operating conditions and turbine control parameters on the SDM are investigated. To strengthen the SSI damping controller performance against communication delays, a Smith predictor scheme is also developed. The effectiveness of the proposed delay analysis framework and Smith predictor scheme based delay immune controller is validated through Electromagnetic Transient (EMT) simulations on a realistic test system with multiple series capacitor compensated lines considering various operation conditions.

INDEX TERMS Doubly-fed induction generator (DFIG), optimal control, series capacitor compensation, stability delay margin, subsynchronous interaction (SSI).

I. INTRODUCTION

Subsynchronous Interaction (SSI) phenomenon includes the situation in which a series capacitor compensated transmission system and doubly-fed induction generator (DFIG)-based wind farm exchange energy in the frequencies below the nominal system frequency [1], [2]. Since the first SSI accident in ERCOT system [3], [4], a significant amount of research is conducted to mitigate the phenomenon particularly by augmenting DFIG control circuit [5]–[15] with supplementary controllers. These controllers are often designed to operate in the secondary control level of the wind farm (i.e. central implementation like wind farm controller) as the entire system inside the wind farm is represented with a single aggregated WT. On the other hand, the central implementation of the SSI damping controller may result in several practical issues such as vulnerability to delays in the feedback control loops [16]. Especially, malfunction of sensors, or cyber-attacks on the communication structure between the wind turbines and the central controller can result in latency in the feedback loops and compromise the system stability.

The stability of a closed-loop realistic system hugely depends on the delay in its control feedback loops [17]. In power system applications, the presence of delay is often ignored for the sake of simplification owing to the practical assumption that the latency of the local measurements is

The associate editor coordinating the review of this manuscript and approving it for publication was Dragan Jovcic.

small. However, the delay may considerably increase in case of complex and widespread communication infrastructures such as those found in wind farms, or in case of cyber-attacks. Therefore, new studies focus on the impact of time delay on the power system stability in several domains, to name a few, the impact on Power System Stabilizer (PSS) [18], FACTS devices such as TCSC [19] and SVC [20], and load frequency control [21]. A sensor/communication link malfunction or a pin prick cyber-attack jamming delays can remain stealthy for a long period of time as it won't be noticeable enough until a large-scale disturbance in the grid occurs.

The value of system latency is often assumed to be a constant value. However, in a realistic system, it is a uniform random number within a range [22]. Therefore, it is essential to obtain the time delay limit that results in system instability when exceeded. This maximum time delay is referred to as stability delay margin (SDM) [23]. Any adversary or malfunction of the sensor/communication system that causes a latency more than the SDM will destabilize the system.

The characteristic equation of a time-delayed system is transcendental, and thus, its stability (i.e., loci of the zeros of the characteristic polynomial) cannot be assessed using the conventional stability evaluation methods. Among the methods that focus on the delay margin computation [24], [25], Rekasius Substitution [25] is a well-established and recognized one. Using this method, the exponential term is replaced by its equivalent transfer function on the imaginary axis of the s-plane. Despite numerous advantages, its large computational burden for the complex and large-scale dynamic systems, such as power systems or wind farms, limits its extensive use.

In this paper, a new algorithm that benefits from the Rekasius Substitution and Guardian Map Theorem [26] is proposed for the accurate calculation of SDM, which indicates the strength level of a system against communication delays. The proposed algorithm reduces the computational burden of the delay margin calculation, and also provides an insight on how close to the instability point a system is in the presence of uncertainty. Then, as an example, the delay vulnerability of a series compensated DFIG-based wind farm, of which SSI modes are mitigated by a central supplementary controller, is investigated using the proposed algorithm. The robust damping controller is designed using μ-technique and implemented in the secondary control level of the wind farm. The input signals of the SSI damping controller are the currents of Rotor Side Converter (RSC) and Grid Side Converter (GSC) in dq-frame. The outputs are added into the inner control loops of DFIG to achieve the maximum possible damping provided by the converter system. The impact of wind farm and power system parameters on the delay margin is investigated using a sensitivity analysis. Such analysis results in obtaining the operating conditions in which the system is more vulnerable to subsynchronous instability in the presence of delay. To increase the SDM of the system and to harden the defense layer, a Smith Predictor scheme is adopted in this manuscript. This predictor scheme removes the delay from the system control loop using the difference between system mathematical model and plant output. The proposed analytical method is validated through Electromagnetic Transient (EMT) simulations with detailed wind farm model. The contributions of this paper can be summarized as:

(i) A novel and efficient framework dedicated for SSI stability margin analysis considering communication delays and parametric uncertainties;
(ii) Detailed case study of the proposed framework applied to a realistic power system with a DFIG-based wind farm connected to a series compensated transmission network; and
(iii) An stability enhancement scheme for SSI control against communication delay based on the Smith Predictor technique.

In this paper, Section II briefly explains the control system of a wind turbine. The test system is given in Section III. The procedure of obtaining delay stability margin is presented in Section IV. In this Section, the impact of various system parameters on the SDM is demonstrated, and obtained results are validated through EMT simulations. Section V introduces the Smith predictor structure and demonstrates its effectiveness through EMT simulations. Section VI presents the conclusions.

II. WIND TURBINE CONTROL

In a wind farm, each DFIG turbine is connected to the Medium Voltage (MV) collector grid typically through a Yg/Delta transformer. The MV collector grid consists of several feeders and connects all DFIG transformers to the wind farm transformer. The wind farm transformer and High Voltage (HV) transmission grid connection is called Point of Interconnection (POI). Each DFIG wind turbine comprises an Induction Generator (IG) and a back-to-back converter system that connects the IG wound rotor to the grid. The control of DFIG converters is based on vector control technique. The main advantage of this technique is the decoupled control of active and reactive converter currents.

The control system of the DFIG is shown in Fig. 1. RSC and GSC are operating in flux and voltage reference frames, respectively. RSC controls the DFIG terminal voltage and active power output. The DFIG active power reference (P'_{dfig}) is provided by the Maximum Power Point Tracking (MPPT) algorithm. The DFIG terminal voltage reference ($1 + \Delta V'_{dfig}$) is modified by the central Wind Farm Controller (WFC) to achieve the desired reactive power at POI. RSC control gives the priority to the active current during normal operation and changes the priority to the reactive current during faults to achieve the grid code compliant operation.

GSC is used to regulate the DC link voltage and it operates at unity factor during normal operation. However, it also injects reactive currents during faults when the RSC reactive current contribution is not sufficient to satisfy the grid code requirement.

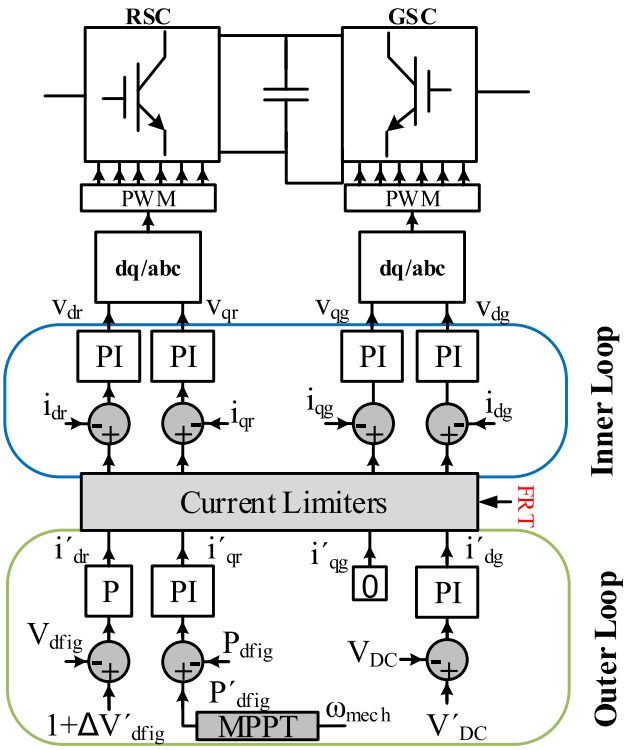

FIGURE 1. The control schematic of the DFIG.

In Fig. 1 and henceforward, all variables are in pu and primed variables are used to indicate the reference values transmitted from controllers. The equations describing the control circuit of the RSC and GSC are

$$\begin{aligned} v'_{dr} &= (K_{Pr} + \frac{K_{Ir}}{s})(i'_{dr} - i_{dr}) + FF_{dr} \\ v'_{qr} &= (K_{Pr} + \frac{K_{Ir}}{s})(i'_{qr} - i_{qr}) + FF_{qr} \\ v'_{dg} &= (K_{Pg} + \frac{K_{Ig}}{s})(i'_{dg} - i_{dg}) + FF_{dg} \\ v'_{qg} &= (K_{Pg} + \frac{K_{Ig}}{s})(i'_{qg} - i_{qg}) + FF_{qg} \end{aligned} \quad (1)$$

where v_{dr} and v_{qr} are d- and q- axis voltages of the RSC, respectively. v_{dg} and v_{qg} indicate the d- and q- axis voltages of GSC, respectively. K_{Pr} and K_{Ir} are the PI control parameters of the RSC, and K_{Pg} and K_{Ig} are the proportional and integral coefficients of the GSC. FF_{dr}, FF_{qr}, FF_{dg} and FF_{qg} are the feedforward signals whose detailed expressions can be found in [27]. The current reference values are:

$$\begin{aligned} i'_{dr} &= K_v(1 + \Delta V'_{dfig} - V_{dfig}) \\ i'_{qr} &= (K_{PP} + \frac{K_{PP}}{s})(P'_{dfig} - P_{dfig}) \\ i'_{dg} &= (K_{Pdc} + \frac{K_{Idc}}{s})(V'_{DC} - V_{DC}) \end{aligned} \quad (2)$$

where K_v is the voltage regulator gain, and K_{PP}, K_{IP}, K_{Pdc} and K_{Idc} are the proportional and integral parameters of the active power and DC voltage controllers.

The linearized model of the simplified system is used to perform the analysis of the SDM. The simplified system is obtained by augmenting the equations of the system components and ignoring the dynamics with marginal impact on the subsynchronous stability. The single line diagram of this simplified system is shown in Fig. 2. In this figure, all the series impedances of the wind farm are added to the transmission line. The obtained linearized model is verified using EMT simulations.

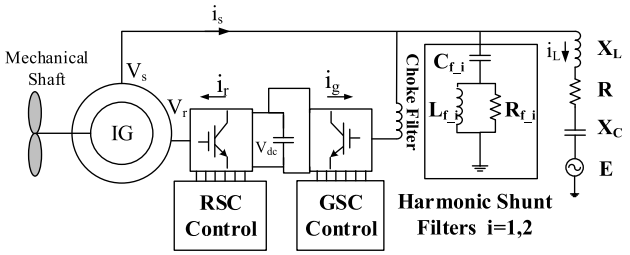

FIGURE 2. Single-line diagram of simplified system.

III. SYSTEM UNDER STUDY

The test system simulated in EMTP [28] is shown in Fig. 3. The wind farm has 266 DFIG wind turbines with 1.5 MW power rating and connected to the power grid (represented with Thevenin equivalents) through the transmission lines A, B and C. Two of these lines (line B and C) are compensated with 50% compensation level using identical capacitor banks at their ends. $B1$, $B2$, $B3$, $\bar{B}1$, $\bar{B}2$ and $\bar{B}3$ are the line circuit-breakers. The operating times of the line circuit-breakers are 60 ms and 80 ms for the close and remote faults, respectively. The SSI mode frequency changes significantly at each line outage scenario [13]. The generic DFIG wind turbine model in [27] is used in simulations. The DFIG wind turbine model includes all the nonlinearities (in both electrical and control system model) and essential transient functions for grid compliant operation. The EMT model of the wind farm contains 266 DFIG wind turbines and detailed medium voltage (MV)

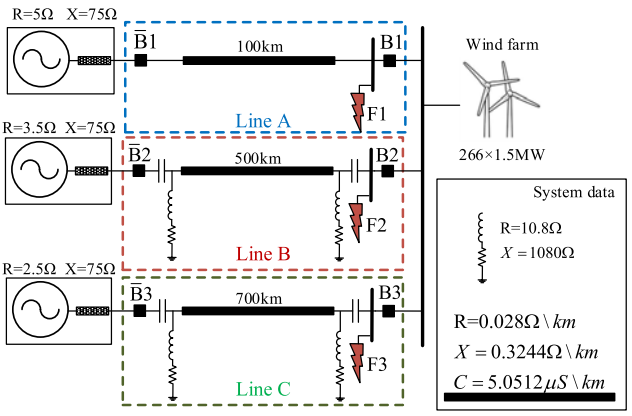

FIGURE 3. The case study system.

collector grid. The DFIG converters are represented with average value models (AVMs) and the simulation time step is 50 μs. Reader should refer to [16] for the details of the EMT model.

The SSI damping controller is designed using μ-technique and DK-iteration method [29] to stabilize the system. The inputs of the controller are the RSC, and GSC currents in the dq-reference frame. The outputs of the controller are connected to the inner loops of both converters. The variation of the power system impedance (moved to the low voltage side of the turbine) is modeled using uncertain resistance, reactance and capacitance values within the state-space representation of the system. Reader should refer to [13] for details of both the test system given in Fig. 3 and the SSI damping controller. This paper considers a central SSI damping controller implementation as illustrated in Fig. 4. In this implementation, each DFIG control system sends the converter current measurements to the central damping controller (α in Fig. 4) and receives the output signal of the central SSI damping controller (β in Fig. 4). As this figure represents, a set of communication links are required to transfer these signals, which consequently makes the scheme prone to delay.

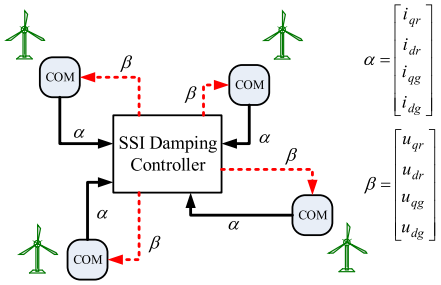

FIGURE 4. Implementation of SSI damping controller and communication signals between control layers.

The simulated fault scenarios are presented in Table 1. They are three-phase metallic faults. The fault locations $F1$, $F2$ and $F3$ are illustrated in Fig. 3. These faults are cleared with the operation of line circuit-breakers.

TABLE 1. Simulation scenarios.

Scenario	Pre-fault condition (line outage)	Post-fault condition (line outage)	Fault time	Fault location
a	-	A	1s	F1
b	A	C	4s	F3
c	A	B	4s	F2

IV. DELAY STUDY

The state-space representation of a linear time-invariant system (e.g., wind farm and power system) can be expressed as:

$$\begin{aligned} \dot{\mathbf{x}} &= \mathbf{A}\mathbf{x} + \mathbf{B}\mathbf{u} \\ \mathbf{y} &= \mathbf{C}\mathbf{x} + \mathbf{D}\mathbf{u} \end{aligned} \tag{3}$$

where $\mathbf{A} \in \mathcal{R}^{n\times n}$, $\mathbf{B} \in \mathcal{R}^{n\times m}$, $\mathbf{C} \in \mathcal{R}^{r\times n}$ and $\mathbf{D} \in \mathcal{R}^{r\times m}$ are the matrices obtained from linearization process and describe the small signal behavior of the linearized system. In this equation, n, m and r represent the size of state, input and output vectors, respectively. $\mathcal{R}$ is the set of matrices in real numbers.

The state-space representation of the designed μ-controller in the secondary level, and the resulted closed-loop system are, respectively, expressed in (4) and (5) as

$$\begin{aligned} \dot{\mathbf{x}_K} &= \mathbf{A_K}\mathbf{x_K} + \mathbf{B_K}\mathbf{y} \\ \mathbf{u} &= \mathbf{C_K}\mathbf{x_K} + \mathbf{D_K}\mathbf{y} \end{aligned} \tag{4}$$

and

$$\begin{bmatrix} \dot{\mathbf{x}} \\ \dot{\mathbf{x}_K} \end{bmatrix} = \begin{bmatrix} \mathbf{A} & \mathbf{B}\mathbf{C_K} \\ 0 & \mathbf{A_K} \end{bmatrix} \begin{bmatrix} \mathbf{x} \\ \mathbf{x_K} \end{bmatrix} + \begin{bmatrix} 0 & 0 \\ \mathbf{B_K}\mathbf{C} & 0 \end{bmatrix} \begin{bmatrix} \mathbf{x}^\tau \\ \mathbf{x_K}^\tau \end{bmatrix} \tag{5}$$

In these equations, K subscript is used to indicate the controller parameters, e.g., $\mathbf{x_K}$ is the state vector of the controller. Fig. 5 shows different control layers of the closed-loop system, where $\mathbf{y}^\tau$ is the vector of delayed measurement signals.

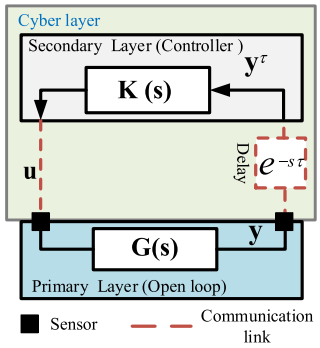

FIGURE 5. The control scheme for analyzing the SDM.

The stability condition of the closed-loop system depends on the location of the roots of the following characteristic equation:

$$\begin{aligned} \Delta(s,\tau) &= det(s\mathbf{I} - \bar{\mathbf{A}} - \bar{\mathbf{A}}_\tau e^{-s\tau}) = \sum_{k=0}^{n} a_k(s) e^{-ks\tau} \\ \bar{\mathbf{A}} &= \begin{bmatrix} \mathbf{A} & \mathbf{B}\mathbf{C_K} \\ 0 & \mathbf{A_K} \end{bmatrix} \\ \bar{\mathbf{A}}_\tau &= \begin{bmatrix} 0 & 0 \\ \mathbf{B_K}\mathbf{C} & 0 \end{bmatrix} \end{aligned} \tag{6}$$

where $a_K(s)$, $k = 0\ldots, n$ are the polynomials in s-plane with real coefficients. Assuming $\gamma_1^\tau, \ldots, \gamma_n^\tau \in \gamma^\tau$ to be the set of the roots of $\Delta(s,\tau)$, the system is small signal stable if and only if:

$$max(real(\gamma_i^\tau)) < 0 \quad \forall \gamma_i^\tau \in \gamma^\tau \tag{7}$$

The aforementioned formulation categorizes the dynamic systems into following types:

(i) Delay independent: if equation (7) is satisfied for all positive values of delay ($\tau \geq 0$), the system is delay independent, and

(ii) Delay dependent: if there exists a value (τ^*) for which the system is stable ((7) is satisfied) for $\tau < \tau^*$ and is not stable for $\tau \geq \tau^*$.

The exponential term ($e^{-k\tau s}$) makes (6) transcendental. Thus, the system stability assessment cannot be performed using the conventional tests. The Rekasius substitution technique replaces the exponential term with an equivalent transfer function. This function describes the exponential term precisely at the imaginary axis of s-plane (i.e., $s = j\omega_c$) as:

$$\tau \in R^+ \quad \text{and} \quad s = j\omega_c \rightarrow e^{-\tau s} = \frac{1 - Ts}{1 + Ts} \quad T \in R \tag{8}$$

It is worth mentioning that the Rekasius substitution is not an approximation technique (such as Pade approximation) since it is accurate and valid only on the imaginary axis. The eigenvalues of the system (i.e., roots of $\Delta(s, \tau)$) should cross the imaginary axis to be on the right half-plane and cause instability, Fig. 6. Thus, at the point of instability, the Rekasius substitution conditions are satisfied.

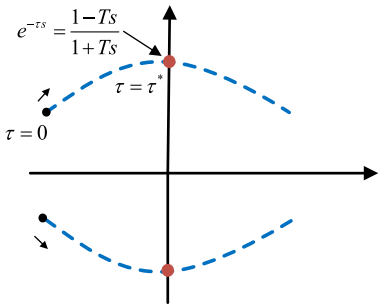

FIGURE 6. The delay equivalence transfer function at Rekasius substitution.

The relation between ω_c and T can be expressed as [25]:

$$\tau = \frac{2}{\omega_c}(tan^{-1}(\omega_c T) \pm i\pi), \quad i = 1, 2, 3, \ldots \tag{9}$$

Substituting (8) into (6), the characteristic equation of the system can be described as:

$$\Delta(s, \tau) = \sum_{k=0}^{n} a_k(s)(\frac{1 - Ts}{1 + Ts})^k \tag{10}$$

To find T which results in $\Delta(s, \tau) = 0$, both sides of the equation (10) are multiplied by $(1 + Ts)^n$, i.e.,

$$\Delta(s, \tau) = \sum_{k=0}^{n} a_k(s)(1 - Ts)^k(1 + Ts)^{n-k} \tag{11}$$

The roots of this polynomial determine the stability of the delayed system. It should be noted that using this technique, the transcendental equation with order n is converted to a polynomial with order $2n$. In this stage, any stability assessment test for linear systems such as Routh's array or root sensitivity methods can be leveraged to conclude on the stability of the system as detailed in [24] and [30]. However, in case of high order and uncertain systems, the use of these methods will result in complexity due to significant increase in the order of the system and presence of unknown parameters T in the equations. Therefore, the Guardian Map Theorem [26] is used to obtain the regions of stability for the parameter T. In the delay analysis of the system, the parameter T is assumed to be an uncertain parameter. Therefore, the problem of obtaining delay stability margin reduces to finding the stability margin of this parameter. The Guardian Map Theorem is a powerful analysis tool for finding the stability state of the uncertain systems [26]. The main advantages of using the Guardian Map Theorem are its simplicity for large-scale systems as well as providing insight about the stability regions.

A. GUARDIAN MAP THEOREM

Assume that the set of all polynomials with degree at most n and real coefficients are represented by X, and let S be an open subset of X. Here, a set is defined to be open if all of its points have a neighborhood contained in the set. Let also ν be a scalar-valued function which maps X into the set of complex numbers C, and assume $\bar{S}$ to be the closure of S in X. The closure of a set is the union of its interior and its boundary. Also, ∂S denotes the boundary of the set S in X. Then, we say ν guards S if, for all $x \in \bar{S}$, the following condition holds:

$$x \in \delta\mathcal{S} \Leftrightarrow \upsilon(x) = 0, \tag{12}$$

In such case, ν is referred to as the guardian map for S. This definition and its subsequent proposition can be used to tackle the robust stability problem of a parameterized family of polynomials [26].

B. PROPOSITION

Assume r to be the set of uncertain parameters, i.e., $r = (r_1, r_2, \ldots, r_i) \in U$, and U is a pathwise connected subset of R^k. Let also $x(r)$ be a matrix or polynomial in X which depends continuously on vector r. Let also $S \subset X$ be guarded by ν and assume that $x(r^0) \in S$ for at least one $r^0 \in U$. Then,

$$x(r) \in \mathcal{S} | \ \forall r \in U \Leftrightarrow \nu(x(r)) \neq 0 | \ \forall r \in U \tag{13}$$

As an example, the set of non-singular square matrices are guarded by the determinant of them. More details and proof of Guardian Map Theorem can be found in [26].

The set of Hurwitz-stable real polynomials of the form $P(s) = q_n s^n + q_{n-1}s^{n-1} + q_{n-2}s^{n-2} + \ldots + q_0$ with uncertain coefficients q_i is guarded by the map $\nu : A \rightarrow detH(P)$ where $H(P)$ is the Hurwitz matrix given by

$$H(P) = \begin{bmatrix} q_{n-1} & q_{n-3} & q_{n-5} & . & . & . & 0 \\ q_n & q_{n-2} & q_{n-4} & . & . & . & . \\ 0 & q_{n-1} & q_{n-3} & . & . & . & . \\ 0 & q_n & q_{n-2} & . & . & . & . \\ 0 & 0 & 0 & . & . & . & . \\ 0 & 0 & 0 & . & . & q_1 & 0 \\ 0 & 0 & 0 & . & . & q_2 & q_0 \end{bmatrix} \tag{14}$$

The Guardian Map Theorem provides the maximum value of T in which the system remains still stable. In summary, the problem of stability assessment of an uncertain parametric

system is converted into finding smallest zero of a polynomial by Guardian Map Theorem.

In the next step, both T and ω_c are obtained and used to calculate τ_i^* according to (9). Then, τ^* (i.e., delay margin) can be obtained as:

$$\tau^* = min(\tau_i^*) \tag{15}$$

The procedure of delay margin calculation is illustrated in Algorithm 1. Fig. 7 - Fig. 14 illustrate the regions of stability considering the variation of the wind speed, RSC rise-time, GSC rise-time, voltage regulation gain (K_v), active power loop gain of RSC (K_P), resistance, reactance, and capacitance observed from DFIG terminal.

Algorithm 1 Proposed Algorithm for Obtaining SDM

1 Obtain the state-space representation of the system and compute $\mathbf{A}$ and $\mathbf{A}_d$ using system equations
2 Obtain $\Delta(s, \tau)$ using (5)
3 Obtain the characteristic polynomial using Rekasius substitution
4 Use the Guardian Map Theorem and calculate the determinant of the Hurwitz matrix $H(P)$
5 Calculate T which results in the system instability
6 Obtain ω_{ci} and τ_i^* using (11) and (8), respectively
7 7. Find the minimum value of τ_i^*s

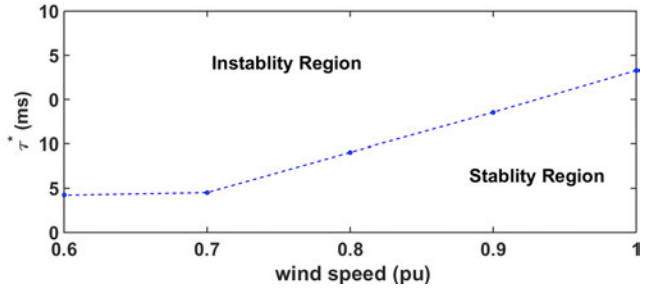

FIGURE 7. Impact of wind speed on the SDM.

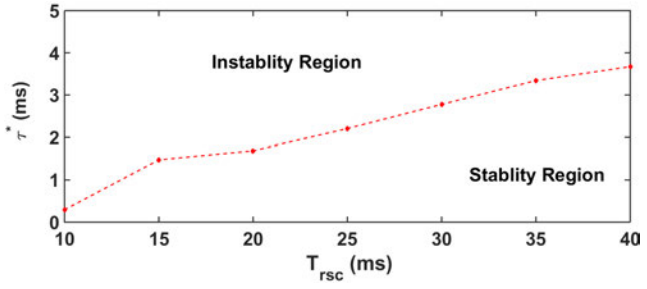

FIGURE 8. Impact of RSC rise-time on the SDM.

The obtained results show that the decrease in wind speed, RSC rise-time and GSC rise-time will result in the increase of SDM. Moreover, the larger the voltage regulation gain and active power loop gain are, the smaller the SDM is. The

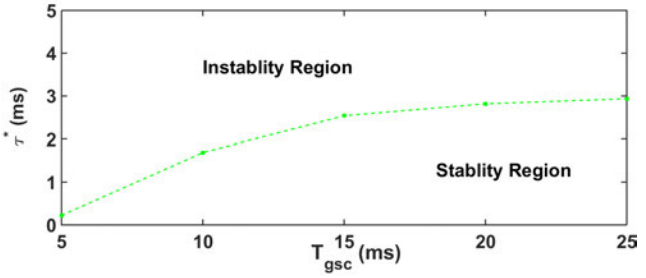

FIGURE 9. Impact of GSC rise-time on the SDM.

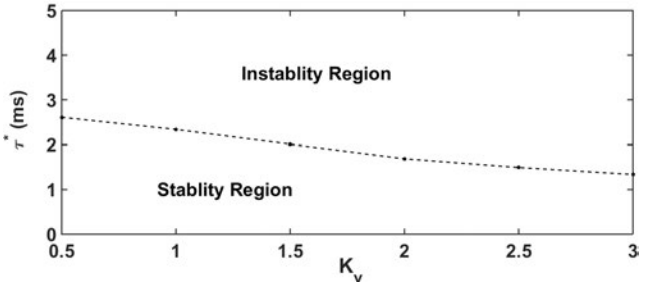

FIGURE 10. Impact of voltage regulation gain on the SDM.

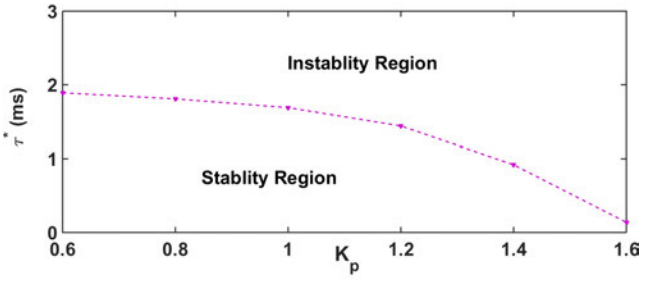

FIGURE 11. Impact of RSC active power loop gain on the SDM.

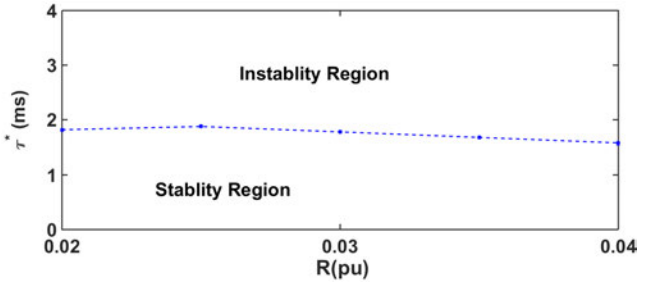

FIGURE 12. Impact of resistance observed from DFIG terminal on the SDM.

external power system parameters has smaller impact on the SDM compared to wind speed and WT control parameters. Fig. 15 - Fig. 17 compare the results obtained from EMT simulations of the delayed and non-delayed systems for scenarios a, b and c, respectively. Typical WT control parameters and the slowest permissible wind speed are considered in these simulations. The calculated SDM are 1.84 ms, 2.49 ms and 2.67 ms for scenarios a, b and c, respectively. The presented

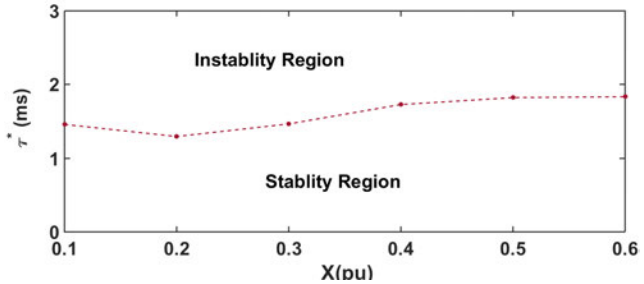

FIGURE 13. Impact of reactance observed from DFIG terminal on the SDM.

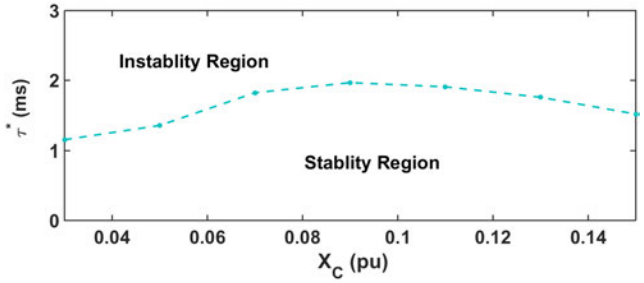

FIGURE 14. Impact of capacitance observed from DFIG terminal on the SDM.

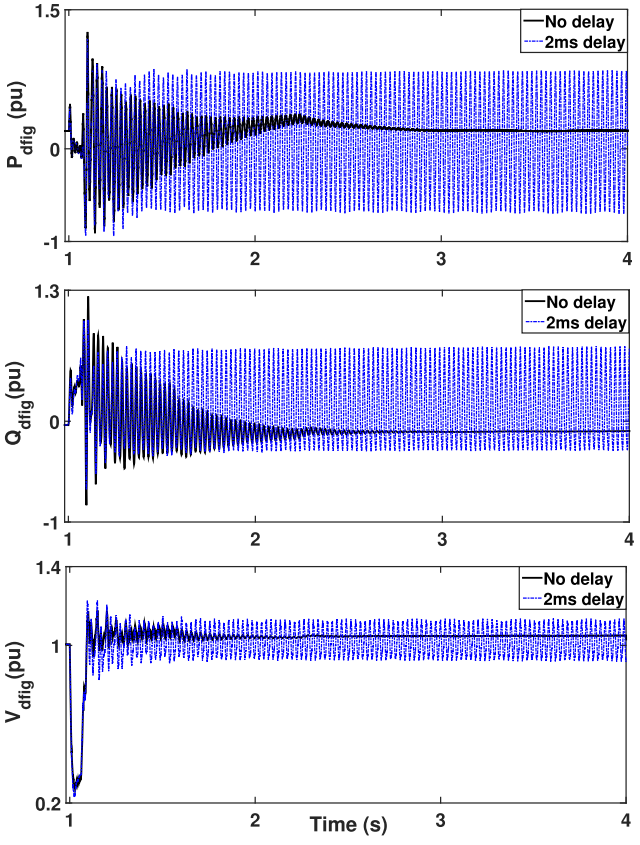

FIGURE 15. P(pu), Q(pu) and V(pu) of the DFIG with and without delay in scenario a.

waveforms in Fig. 15 - Fig. 17 demonstrate the instability due to communication delays and confirm the proposed stability delay analysis.

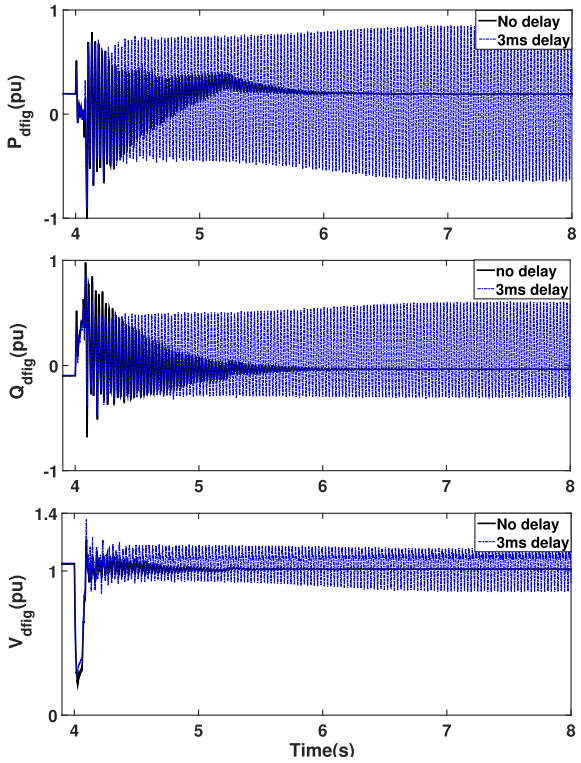

FIGURE 16. P(pu), Q(pu) and V(pu) of the DFIG with and without delay, scenario b.

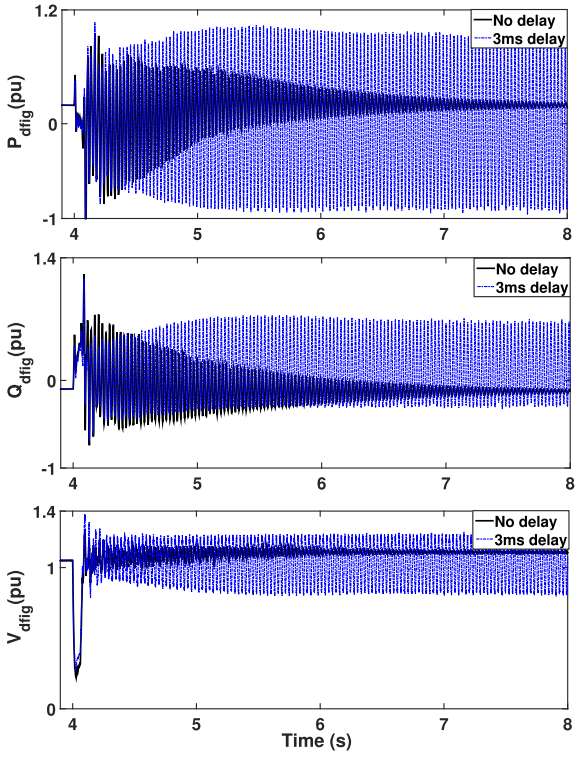

FIGURE 17. P(pu), Q(pu) and V(pu) of the DFIG with and without delay, scenario c.

V. SMITH PREDICTOR

To attenuate the negative impact of delay on the behavior of the SSI damping controller and harden the defense layer

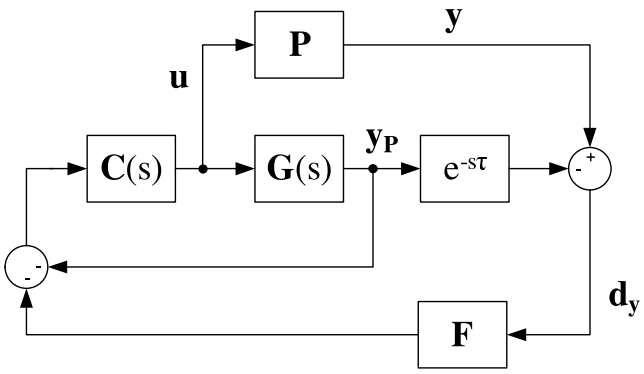

FIGURE 18. The scheme of smith predictor.

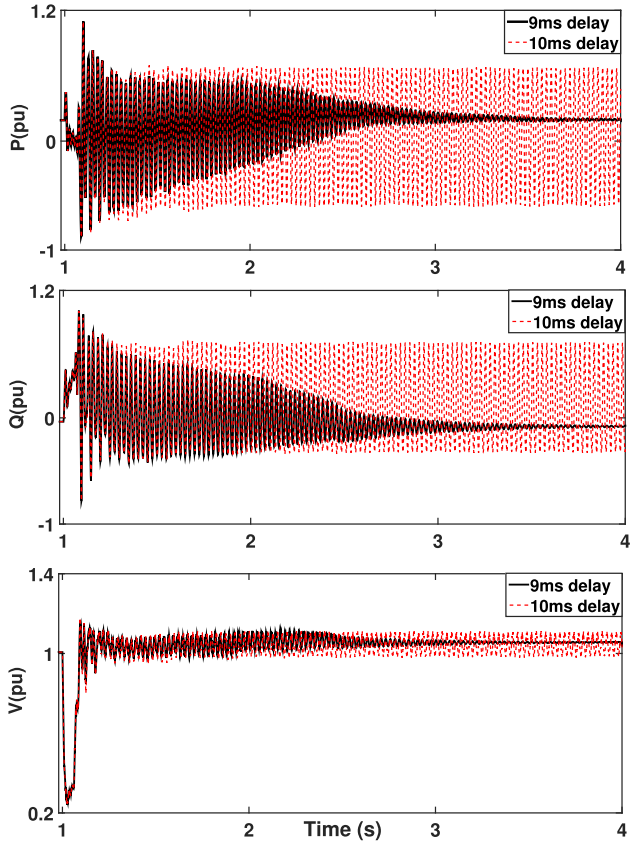

FIGURE 19. The active power, reactive power and terminal voltage of the DFIG using smith predictor, scenario a.

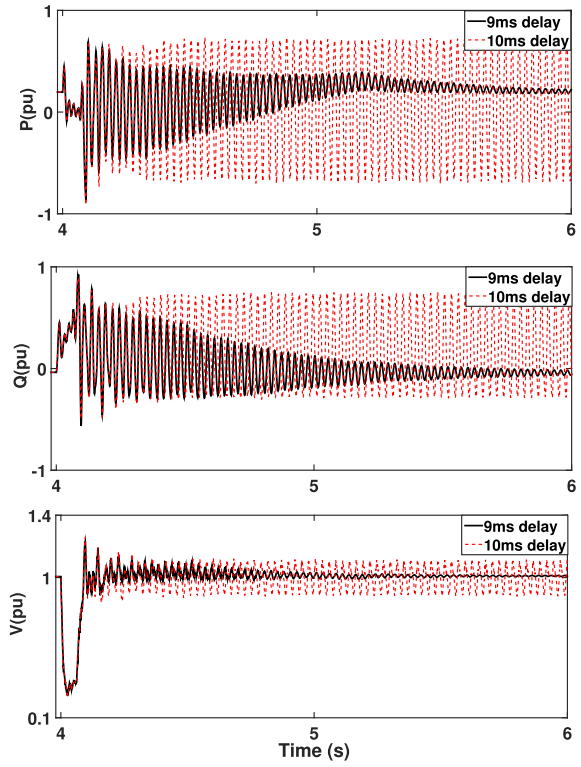

FIGURE 20. The active power, reactive power and terminal voltage of the DFIG using smith predictor, scenario b.

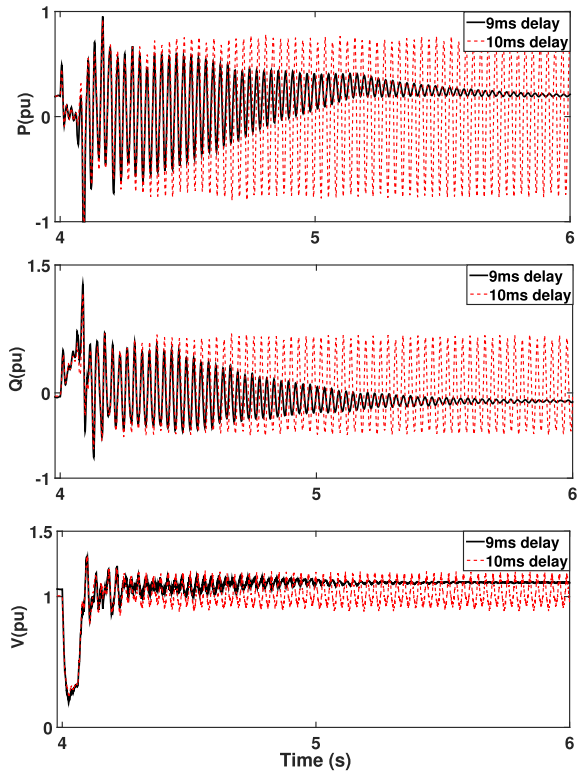

FIGURE 21. The active power, reactive power and terminal voltage of the DFIG using smith predictor, scenario c.

of the cyber system, a new control scheme based on the Smith Predictor is proposed, Fig. 18. In such scheme, **P** is the detailed plant model in EMT simulation environment, $\mathbf{G}(s)$ is the linearized mathematical model of the system, $\mathbf{C}(s)$ is the controller designed using μ-technique, and **F** is a filter used to ensure stability of the Smith predictor. The stability of the predictor scheme as well as the system performance against uncertainty in system parameter or delay value can be modified using the parameters of this filter [31], [32]. The Smith predictor uses the mathematical model of the system to predict the measurement signals in which the delay is zero ($\mathbf{y}_P$). Then, the measurement signal ($\mathbf{y}$) is compared with the delayed output of the linearized model ($\mathbf{y}_1$). The difference between these signals ($\mathbf{y_d}$) is fed back through the filter and

contributes to the input of controller. The filter **F** is designed using several time-domain simulations as:

$$\mathbf{F}(s) = \begin{pmatrix} f & 0 & 0 & 0 \\ 0 & f & 0 & 0 \\ 0 & 0 & f & 0 \\ 0 & 0 & 0 & f \end{pmatrix} \quad f = \frac{5}{(s + 2\pi(20))} \tag{16}$$

Several EMT simulations are performed to demonstrate the effectiveness of the proposed prediction scheme. The positive sequence voltage of the DFIG, and the injected power components are shown in Fig. 19 - Fig. 21. It can be observed that the Smith Predictor can increase the delay stability margin of the system from 2 ms to 9 ms.

VI. CONCLUSION

This paper delivered a systematic detailed analysis on the impact of communication delays on wind farm SSI damping controller performance for the first time. To obtain the impact of different wind farm operating conditions and WT control parameters on the delay stability margin, a new algorithm was proposed based on the Rekasius substitution and Guardian Map Theorem. The proposed algorithm significantly reduces the computational burden of the delay margin calculation for high order systems, e.g., wind farms. The detailed analysis demonstrated that depending on WT control parameters and wind farm operating conditions, a significant performance deterioration in SSI damping controller can be expected due to communication delays (at practical ranges). This paper also proposed a Smith Predictor scheme based controller to extend the stability regions and improve the system response. The proposed approach made the system immune to the excessive (even unrealistic) communication delays. The accuracy of the proposed delay margin analysis and effectiveness of the proposed communication delay immune controller is validated through EMT simulations on a detailed and realistic test system.

REFERENCES

[1] L. Fan, C. Zhu, Z. Miao, and M. Hu, "Modal analysis of a DFIG-based wind farm interfaced with a series compensated network," *IEEE Trans. Energy Convers.*, vol. 26, no. 4, pp. 1010–1020, Dec. 2011.

[2] J. Shair, X. Xie, L. Wang, W. Liu, J. He, and H. Liu, "Overview of emerging subsynchronous oscillations in practical wind power systems," *Renew. Sustain. Energy Rev.*, vol. 99, pp. 159–168, Jan. 2019. [Online]. Available: https://www.sciencedirect.com/science/article/pii/S1364032118306956

[3] B. Badrzadeh, M. Sahni, D. Muthumuni, Y. Zhou, and A. Gole, "Sub-synchronous interaction in wind power plants—Part I: Study tools and techniques," in *Proc. IEEE Power Energy Soc. Gen. Meeting*, Jul. 2012, pp. 1–9.

[4] M. Sahni, B. Badrzadeh, D. Muthumuni, Y. Cheng, H. Yin, S.-H. Huang, and Y. Zhou, "Sub-synchronous interaction in wind power plants—Part II: An ercot case study," in *Proc. IEEE Power Energy Soc. Gen. Meeting*, Jul. 2012, pp. 1–9.

[5] A. E. Leon and J. A. Solsona, "Sub-synchronous interaction damping control for DFIG wind turbines," *IEEE Trans. Power Syst.*, vol. 30, no. 1, pp. 419–428, Jan. 2015.

[6] U. Karaagac, S. O. Faried, J. Mahseredjian, and A.-A. Edris, "Coordinated control of wind energy conversion systems for mitigating subsynchronous interaction in DFIG-based wind farms," *IEEE Trans. Smart Grid*, vol. 5, no. 5, pp. 2440–2449, Sep. 2014.

[7] P.-H. Huang, M. El Moursi, W. Xiao, and J. Kirtley, "Subsynchronous resonance mitigation for series-compensated DFIG-based wind farm by using two-degree-of-freedom control strategy," *IEEE Trans. Power Syst.*, vol. 30, no. 3, pp. 1442–1454, May 2015.

[8] M. A. Chowdhury, M. A. Mahmud, W. Shen, and H. R. Pota, "Nonlinear controller design for series-compensated DFIG-based wind farms to mitigate subsynchronous control interaction," *IEEE Trans. Energy Convers.*, vol. 32, no. 2, pp. 707–719, Jun. 2017.

[9] H. A. Mohammadpour, A. Ghaderi, H. Mohammadpour, and E. Santi, "SSR damping in wind farms using observed-state feedback control of DFIG converters," *Electr. Power Syst. Res.*, vol. 123, pp. 57–66, Jun. 2015.

[10] H. A. Mohammadpour and E. Santi, "Optimal adaptive sub-synchronous resonance damping controller for a series-compensated doubly-fed induction generator-based wind farm," *IET Renew. Power Generat.*, vol. 9, no. 6, pp. 669–681, Aug. 2015.

[11] J. Taherahmadi, M. Jafarian, and M.-N. Asefi, "Using adaptive control in DFIG-based wind turbines to improve the subsynchronous oscillations of nearby synchronous generators," *IET Renew. Power Gener.*, vol. 11, no. 2, pp. 362–369, 2017.

[12] M. Ghafouri, U. Karaagac, H. Karimi, S. Jensen, J. Mahseredjian, and S. O. Faried, "An LQR controller for damping of subsynchronous interaction in DFIG-based wind farms," *IEEE Trans. Power Syst.*, vol. 32, no. 6, pp. 4934–4942, Nov. 2017.

[13] M. Ghafouri, U. Karaagac, H. Karimi, and J. Mahseredjian, "Robust subsynchronous interaction damping controller for DFIG-based wind farms," *J. Mod. Power Syst. Clean Energy*, vol. 7, no. 6, pp. 1663–1674, 2019.

[14] J. Shair, X. Xie, and G. Yan, "Mitigating subsynchronous control interaction in wind power systems: Existing techniques and open challenges," *Renew. Sustain. Energy Rev.*, vol. 108, pp. 330–346, Jul. 2019. [Online]. Available: https://www.sciencedirect.com/science/article/pii/S1364032119302060

[15] J. Shair, X. Xie, Y. Li, and V. Terzija, "Hardware-in-the-loop and field validation of a rotor-side subsynchronous damping controller for a series compensated DFIG system," *IEEE Trans. Power Del.*, vol. 36, no. 2, pp. 698–709, Apr. 2021.

[16] M. Ghafouri, U. Karaagac, J. Mahseredjian, and H. Karimi, "SSCI damping controller design for series-compensated DFIG-based wind parks considering implementation challenges," *IEEE Trans. Power Syst.*, vol. 34, no. 4, pp. 2644–2653, Jul. 2019.

[17] E. Fridman, *Introduction to Time-Delay Systems: Analysis and Control*. Basel, Switzerland: Springer, 2014.

[18] H. Wu, K. S. Tsakalis, and G. T. Heydt, "Evaluation of time delay effects to wide-area power system stabilizer design," *IEEE Trans. Power Syst.*, vol. 19, no. 4, pp. 1935–1941, Nov. 2004.

[19] J. Quanyuan, Z. Zhenyu, and C. Yijia, "Wide-area TCSC controller design in consideration of feedback signals' time delays," in *Proc. IEEE Power Eng. Soc. Gen. Meeting*, Jun. 2005, pp. 1676–1680.

[20] M. S. Saad, M. A. Hassouneh, E. H. Abed, and A.-A. Edris, "Delaying instability and voltage collapse in power systems using SVCs with washout filter-aided feedback," in *Proc. Amer. Control Conf.*, 2005, pp. 4357–4362.

[21] S. Sönmez, S. Ayasun, and C. O. Nwankpa, "An exact method for computing delay margin for stability of load frequency control systems with constant communication delays," *IEEE Trans. Power Syst.*, vol. 31, no. 1, pp. 370–377, Jan. 2016.

[22] S.-I. Niculescu, *Delay Effects on Stability: A Robust Control Approach*, vol. 269. London, U.K.: Springer, 2001.

[23] R. H. Middleton and D. E. Miller, "On the achievable delay margin using LTI control for unstable plants," *IEEE Trans. Autom. Control*, vol. 52, no. 7, pp. 1194–1207, Jul. 2007.

[24] H. Jia, N. Guangyu, S. T. Lee, and P. Zhang, "Study on the impact of time delay to power system small signal stability," in *Proc. IEEE Medit. Electrotech. Conf. (MELECON)*, May 2006, pp. 1011–1014.

[25] N. Olgac and R. Sipahi, "An exact method for the stability analysis of time-delayed linear time-invariant (LTI) systems," *IEEE Trans. Autom. Control*, vol. 47, no. 5, pp. 793–797, May 2002.

[26] L. Saydy, A. L. Tits, and E. H. Abed, "Guardian maps and the generalized stability of parametrized families of matrices and polynomials," *Math. Control Signals Syst.*, vol. 3, no. 4, pp. 345–371, Dec. 1990.

[27] U. Karaagac, H. Saad, J. Peralta, and J. Mahseredjian, "Doubly-fed induction generator based wind park models in EMTP-RV," Ecole Polytechnique Montreal, Montreal, QC, Canada, Res. Rep., 2015.

[28] J. Mahseredjian, S. Dennetière, L. Dubé, B. Khodabakhchian, and L. Gérin-Lajoie, "On a new approach for the simulation of transients in power systems," *Electr. Power Syst. Res.*, vol. 77, no. 11, pp. 1514–1520, Sep. 2007.
[29] D.-W. Gu, P. Petkov, and M. M. Konstantinov, *Robust Control Design With MATLAB*. London, U.K.: Springer, 2005.
[30] H. Jia, X. Cao, X. Yu, and P. Zhang, "A simple approach to determine power system delay margin," in *Proc. IEEE Power Eng. Soc. Gen. Meeting*, Jun. 2007, pp. 1–7.
[31] C. Ahumada, R. Cárdenas, D. Sáez, and J. M. Guerrero, "Secondary control strategies for frequency restoration in islanded microgrids with consideration of communication delays," *IEEE Trans. Smart Grid*, vol. 7, no. 3, pp. 1430–1441, May 2016.
[32] K. Watanabe and M. Ito, "A process-model control for linear systems with delay," *IEEE Trans. Autom. Control*, vol. AC-26, no. 6, pp. 1261–1269, Dec. 1981.

MOHSEN GHAFOURI (Member, IEEE) received the B.Sc. and master's degrees in electrical engineering from the Sharif University of Technology, Tehran, Iran, in 2009 and 2011, respectively, and the Ph.D. degree in electrical engineering from Polytechnique Montréal, Montreal, QC, Canada, in 2018. He was a Researcher with the Iranian Power System Research Institute, Sharif University of Technology, from 2011 to 2014. In 2018, he was a Researcher with CYME International, Eaton Power System Solutions, Montreal. In August 2018, he joined as the Horizon Postdoctoral Fellow with the Security Research Group, Concordia University, where he is currently an Assistant Professor. His research interests include cybersecurity of smart grids, power system modeling, microgrid, wind energy, and control of industrial processes.

ULAS KARAAGAC (Member, IEEE) received the B.Sc. and M.Sc. degrees in electrical and electronics engineering from the Middle East Technical University, Ankara, Turkey, in 1999 and 2002, respectively, and the Ph.D. degree in electrical engineering from Polytechnique Montréal, Montreal, QC, Canada, in 2011. He was a Research and Development Engineer with the Information Technology and Electronics Research Institute (BILTEN), Scientific and Technical Research Council of Turkey (TUBITAK), from 1999 to 2007. He was also a Postdoctoral Fellow with Polytechnique Montréal, from 2011 to 2013, and a Research Associate, from 2013 to 2016. In 2017, he joined the Department of Electrical Engineering, The Hong Kong Polytechnic University, as a Research Assistant Professor. His research interests include integration of large-scale renewables into power grids, modeling and simulation of large-scale power systems, and power system dynamics and control.

ILHAN KOCAR (Senior Member, IEEE) received the B.S. and M.Sc. degrees in electrical engineering from Orta Do u Teknik Üniversitesi, Ankara, Turkey, in 1998 and 2003, respectively, and the Ph.D. degree from Polytechnique Montréal, Canada, in 2009. He worked as a Project Engineer in power electronics with Aselsan Defense Electronics Inc., Ankara, from 1998 to 2004. He worked as a Distribution Software Research and Development Engineer with CYME International T&D, St-Bruno, Canada, from 2009 to 2011. In 2011, he joined the Faculty at Polytechnique Montréal, where he is currently a Full Professor.

ZHAO XU (Senior Member, IEEE) received the B.Eng. degree from Zhejiang University, Hangzhou, China, in 1996, the M.Eng. degree from the National University of Singapore, Singapore, in 2002, and the Ph.D. degree from The University of Queensland, Brisbane, Australia, in 2006. He is currently a Professor with The Hong Kong Polytechnic University, Hong Kong. He was previously with the Centre for Electric Power and Energy, Technical University of Denmark. His research interests include demand side, grid integration of renewable energies and EVs, electricity market planning and management, and AI applications in power engineering. He is also an Editor of the IEEE TRANSACTIONS ON SMART GRID, the IEEE POWER ENGINEERING LETTERS, and the *Electric Power Components and Systems* journal. He is also the Chairman of the IEEE Hong Kong Joint Chapter of IES/IAS/PES/PELS.

EVANGELOS FARANTATOS (Senior Member, IEEE) received the Diploma degree in electrical and computer engineering from the National Technical University of Athens, Athens, Greece, in 2006, and the M.S. and Ph.D. degrees from the Georgia Institute of Technology, Atlanta, GA, USA, in 2009 and 2012, respectively. He is currently a Senior Technical Leader with the Grid Operations and Planning Research and Development Group, EPRI, Palo Alto, CA, USA. He is also managing and leading the technical work of various research and development projects related to synchrophasor technology, power systems monitoring and control, power systems stability and dynamics, system protection, state estimation, renewable energy resources modeling, DER integration, and grid operation with high levels of inverter-based resources. In Summer 2009, he was an Intern at MISO.